



k_{eff} uncertainty quantification and analysis due to nuclear data during the full lifetime burnup calculation for a small-sized prismatic high temperature gas-cooled reactor

Rong-Rui Yang¹ · Yuan Yuan² · Chen Hao^{1,2} · Ji Ma¹ · Guang-Hao Liu¹

Received: 19 July 2021 / Revised: 13 September 2021 / Accepted: 15 September 2021 / Published online: 18 November 2021
© The Author(s), under exclusive licence to China Science Publishing & Media Ltd. (Science Press), Shanghai Institute of Applied Physics, the Chinese Academy of Sciences, Chinese Nuclear Society 2021

Abstract To benefit from recent advances in modeling and computational algorithms, as well as the availability of new covariance data, sensitivity and uncertainty analyses are needed to quantify the impact of uncertain sources on the design parameters of small prismatic high-temperature gas-cooled reactors (HTGRs). In particular, the contribution of nuclear data to the k_{eff} uncertainty is an important part of the uncertainty analysis of small-sized HTGR physical calculations. In this study, a small-sized HTGR designed by China Nuclear Power Engineering Co., Ltd. was selected for k_{eff} uncertainty analysis during full lifetime burnup calculations. Models of the cold zero power (CZP) condition and full lifetime burnup process were constructed using the Reactor Monte Carlo Code RMC for neutron transport calculation, depletion calculation, and sensitivity and uncertainty analysis. For the sensitivity analysis, the Contribution-Linked eigenvalue sensitivity/Uncertainty estimation via Track length importance Characterization (CLUTCH) method was applied to obtain sensitive information, and the “sandwich” method was used to quantify the k_{eff} uncertainty. We also compared the k_{eff} uncertainties

to other typical reactors. Our results show that ^{235}U is the largest contributor to k_{eff} uncertainty for both the CZP and depletion conditions, while the contribution of ^{239}Pu is not very significant because of the design of low discharge burnup. It is worth noting that the radioactive capture reaction of ^{28}Si significantly contributes to the k_{eff} uncertainty owing to its specific fuel design. However, the k_{eff} uncertainty during the full lifetime depletion process was relatively stable, only increasing by 1.12% owing to the low discharge burnup design of small-sized HTGRs. These numerical results are beneficial for neutronics design and core parameters optimization in further uncertainty propagation and quantification study for small-sized HTGR.

Keywords Small-sized HTGR · SU analysis · Nuclear data · Burnup

1 Introduction

Owing to their significant inherent safety and applicability characteristics, high-temperature gas-cooled reactors (HTGRs) have gradually played indispensable roles in nuclear reactor development [1–3]. HTGRs can be split into two types based on their core design: pebble-bed HTGRs, such as the high-temperature reactor pebble-bed module (HTR-PM) developed in China [4], and prismatic HTGRs, such as the modular high-temperature gas-cooled reactor (MHTGR-350), developed in the US [5]. Simultaneously, small reactors have become a hotspot in international nuclear energy research. HTGR technology is developing rapidly in China, and a new small-sized prismatic HTGR is under development by the China Nuclear Power Engineering Co., Ltd. The continued development

This work was supported by the National Natural Science Foundation of China (No. 12075067) and the National Key R&D Program of China (No. 2018YFE0180900).

✉ Chen Hao
haochen.heu@163.com

¹ Fundamental Science on Nuclear Safety and Simulation Technology Laboratory, College of Nuclear Science and Technology, Harbin Engineering University, Harbin 150001, China

² Department of Reactor Technology, Beijing Institute of Nuclear Engineering, China Nuclear Power Engineering Co., Ltd, Beijing 100089, China

of HTGRs requires verification of their designs with reliable high-fidelity physics models and efficient accurate codes. The predictive capability of codes for HTGR designs can be assessed using sensitivity and uncertainty (SU) analysis methods. Through advancements in computer modeling and computational algorithms, as well as the accessibility of new covariance data, SU analysis can quantify the impact of uncertainties on the design parameters of small prismatic HTGRs. In particular, the effective multiplication factor (k_{eff}) is the most important parameter in reactor physical analysis, its uncertainty propagated by nuclear data is usually indicated as an interval of k_{eff} value. Because the uncertainty of nuclear data exists naturally, the contributions of nuclear data on the k_{eff} uncertainty are essential for the designer to optimize core lifetime and neutronics design.

For SU analysis of HTGRs, a representative international project is the Coordinated Research Project (CRP) on the HTGR Uncertainty Analysis in Modeling (UAM), supported by the International Atomic Energy Agency (IAEA), which considers the peculiarities of HTGR designs and simulation requirements [6, 7]. In the CRP, the coupled HTGR system calculations are divided into several steps, each of which can contribute to the total uncertainty. Simultaneously, the input, output, and assumptions for each step need to be identified. The resulting uncertainty in each step is calculated by considering all sources of uncertainties, including related uncertainties from previous steps [8]. Some in-depth studies have quantified the contribution of cross-section uncertainties to the eigenvalue uncertainty for some representative but simplified models for both the pebble-bed and prismatic HTGRs [6–10]. For SU analysis of the prismatic HTGR, local and global calculations have been performed, including steady-state and depletion calculations for the cell and core models. The k_{eff} uncertainties due to the nuclear data for the fresh block core and mixed core of the MHTGR-350 have been quantified [11]. Although both the small-sized HTGR selected in this study and MHTGR-350 belong to prismatic HTGRs, there are some significant differences. Unlike the mixed core arrangement in MHTGR-350, the small-sized prismatic HTGR only has fresh fuel with burnable poison (BP) in the core at the beginning of life (BOL). At the same time, this study can enrich the content of the IAEA CRP in HTGRs.

This study focuses on k_{eff} uncertainty analysis due to the nuclear data during full lifetime burnup calculations of the small-sized prismatic HTGR. We will quantify the different cross-sectional contributions on the k_{eff} uncertainty at the CZP condition and the full lifetime burnup process and analyze the mechanism in-depth. The following section describes the model details of the small-sized prismatic HTGR and SU analysis methods. Based on the first-order

perturbation theory [12], we selected the contribution-linked eigenvalue sensitivity/uncertainty estimation via track length importance characterization (CLUTCH) method [13] to perform the sensitivity analysis, and the “sandwich” rule [14] to quantify the k_{eff} uncertainty by using the ENDF/B-VII.1 based covariance data [23].

The rest of this paper is structured as follows. In Sect. 2, we introduce the model and method applied in this study, especially the full core burnup model of the small-sized HTGR for neutron transport and depletion calculations. In Sect. 3, we present the SU analysis of k_{eff} due to nuclear data in the full lifetime depletion calculation. In Sect. 4, we present the in-depth mechanism analysis of nuclear data contributions on k_{eff} during the full lifetime burnup process. Finally, we present the numerical results and conclusions drawn from SU in Sect. 5.

2 Models and methodologies

2.1 Small-sized HTGR model

The small-sized HTGR, which is under development by the China Nuclear Power Engineering Co., Ltd., was selected as the research target in this study. This small-sized HTGR is a helium-cooled, graphite-moderated prismatic reactor and has some unique characteristics, such as fuel blocks and a burnable poison rod arrangement [15]. A representation of the core layout is shown in Fig. 1; 30 hexagonal prism fuel blocks and 13 control rod blocks are closely arranged in the core. The seven control rod blocks are surrounded by fuel assemblies, including one center startup control block and six shutdown control blocks. The other six control blocks are on the six corners of the core beside the fuel blocks, and each fuel block contains 24 fuel rods and seven coolant channels within the graphite matrix. Each fuel rod or coolant channel has a hexagonal graphite

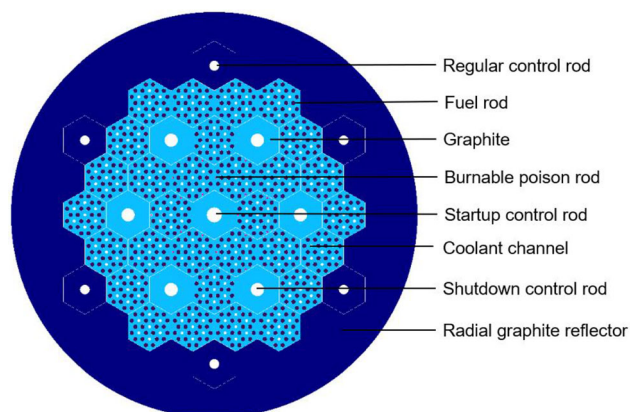


Fig. 1 (Color online) Small-sized prismatic HTGR cross-sectional layout

cladding in the fuel blocks. The radial reflector around the core is also made of graphite, but the density is much lower than the hexagonal graphite cladding. The coolant gas and reflector material specifications are the same as those of the pebble bed reactor, which uses helium as the coolant and graphite as the moderator and reflector. In particular, several cylinder fuel pellets are added to the upper and bottom reflective layers to constitute a fuel rod and TRISO particles [16] are dispersed in the SiC matrix to form a fuel pellet. This is different from the pebble-bed HTGR, in which TRISO particles are dispersed in the graphite matrix.

During the burnup calculation, every fuel kernel in the TRISO particles is a basic burnup unit. At the same time, as the depletion proceeds, fission nuclides are consumed and new fission products, such as Ce, Pr, Pu, and Np, are generated. Some of these will cause fission events again and introduce new uncertainties to the core. Moreover, owing to the arrangement of the reflective layers, fuel blocks, and control rod blocks presented in Fig. 1, the discrepancy in the burnup degree in different burnup areas will be gradually evident during the depletion process. Thus, a 24 burnup zone model (four zones in the radial direction and six zones in the axial direction) was established for the depletion calculation, as shown in Fig. 2.

In this study, the reactor Monte Carlo code (RMC), developed by Tsinghua University, was used for calculating the neutron transport and depletion for the high-fidelity model of the small-sized prismatic HTGR [17]. The ENDF/B-VII.1 cross-section library [23] was chosen for the calculation. The setting parameters for the MC critical and

burnup calculations are illustrated in Table 1. Based on these parameters, each MC critical calculation for this model can converge and fulfill the accuracy requirements of the calculated results. For the full core depletion calculation, the statistical error-based MC method was lower than 25 pcm in each burnup step. At the same time, fission poisons, such as ^{135}Xe and ^{149}Sm , can have a huge impact on reactivity at the BOL. Therefore, to study these nuclide reaction contributions to k_{eff} uncertainty and its sensitivity variation during the burnup calculation, the time of the burnup steps must be set small at the BOL, as illustrated in Table 1. During the depletion calculation, the RMC produces a large amount of complicated nuclide information, including the nuclide densities for each burnup region in each burnup step. In addition, the predictor correction method was used for the RMC burnup calculation [18]. For the MC depletion calculation, the nuclide densities used for this burnup step were derived from the results of the previous burnup step. Therefore, the densities of the nuclides as the input parameters for the uncertainty calculation should be the average value of the predicted and corrected densities [19].

Moreover, because all fresh fuels are input into the core simultaneously, there is a large amount of excess reactivity at the BOL. BP isotopes, such as ^{157}Gd , ^{10}B , or ^{167}Er , have large neutron absorption cross-section of themselves and little absorption cross-section of their products, which usually be chosen to balance the excessive reactivity at BOL to reduce the number of control rods as well as deepen the burnup and flatten the distribution of neutron fluence rate. For this burnup model, there are six center fuel blocks around the center control rod block, each containing three Gd_2O_3 burnable poison rods, each of which is a unique burnup unit during the MC depletion calculation.

2.2 SU analysis method

In this paper, the CLUTCH method [13] based on first-order perturbation theory was used for k_{eff} sensitivity analysis during the Monte Carlo calculations. This method calculates the importance of events during a particle's lifetime by examining the number of fission neutrons created by that particle after those events occur. The aim is to produce an accurate and efficient method for calculating k_{eff} sensitivity coefficients for nuclear cross-sections with a relatively small computational memory.

The CLUTCH method only calculates the sensitivity information during the forward calculations. Therefore, a fine important weight function $F^*(r)$ mesh number should be set to ensure accurate sensitivity. An interval of 1–2 cm mesh is typical for obtaining accurate $F^*(r)$ estimates [13]. The $F^*(r)$ mesh only needs to cover the fissionable regions in the core; therefore, in this study, the mesh only needed to

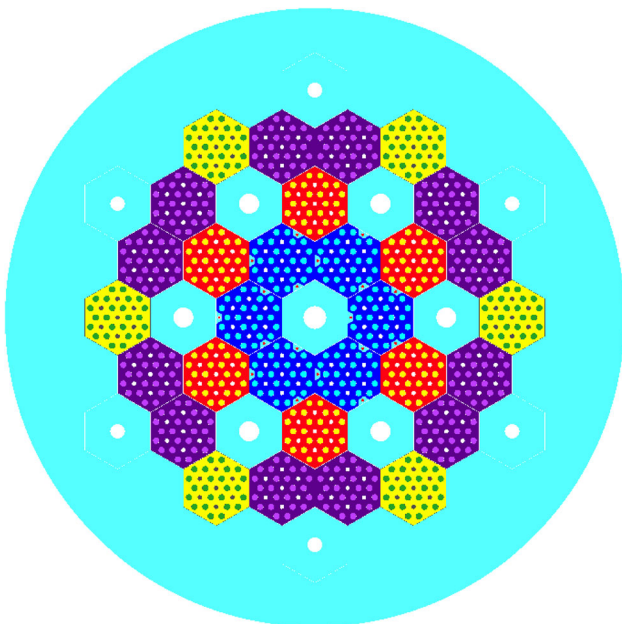


Fig. 2 (Color online) Schematic depletion areas of the small-sized HTGR

Table 1 Monte Carlo neutron transform and depletion calculation setting parameters in RMC

Number of total generations	150
Inactive generations	50
Number of neutrons per generation	100,000
Burnup steps	15
Burnup sub-steps	10
Burnup step time (day)	0.5, 1.0, 3.5, 15, 30, 50 × 7, 100 × 2

cover the fuel block regions. The $F^*(r)$ meshes are also calculated in the inactive generations, so at least 50 to 100 inactive histories should be simulated per mesh interval for sufficient $F^*(r)$ convergence. In this paper, 1.8 cm length meshes in radial, 1.86 cm length meshes in axial, and 750 total histories and 600 inactive histories were set for the CLUTCH method calculations. After the sensitivity coefficients were measured by the CLUTCH method, the k_{eff} uncertainty can be quantified using the “sandwich” rule [14] and the ENDF/B-VII.1 based covariance matrix [23].

3 SU analysis of k_{eff} during the full lifetime depletion calculation

3.1 SU analysis of k_{eff} at CZP condition

Based on the RMC depletion calculation, several burnup step results were chosen to investigate the uncertainty of k_{eff} due to nuclear data. At the BOL, there is only fresh fuel in the core and no fission products, which is known as the cold zero power (CZP) condition. To observe the sensitivity and uncertainty contribution of key nuclide cross sections in the depletion process, SU analysis at the CZP condition should be considered. Through uncertainty quantification, the relative standard deviation of k_{eff} due to nuclear data at the CZP condition was 0.6586%. The top 10 most crucial nuclide reaction covariance contributors to the k_{eff} uncertainty for small-sized HTGRs under the CZP

condition are presented in Table 2, where the numerical results were obtained by RMC.

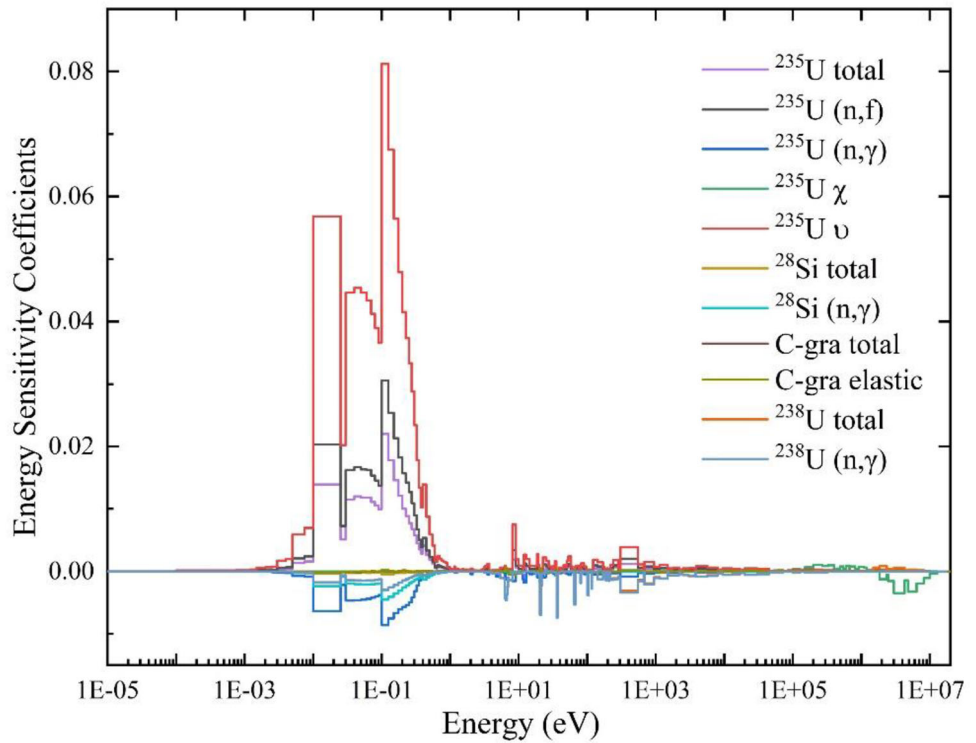
The average number of neutrons emitted per fission event of ^{235}U is the main contributor to the k_{eff} uncertainty and accounts for nearly 17.40% of the total uncertainty of k_{eff} -based nuclear data. This phenomenon is similar to the results of a previously reported uncertainty analysis of HTR-10 [10, 22]. However, the main k_{eff} uncertainty contributors from the results of uncertainty analyses of typically pressurized water reactors (PWRs) and boiling water reactors (BWRs) [20, 21] are different, which has detailed description in Sect. 3.2.2. Moreover, the radioactive capture reaction cross-section of ^{28}Si should be considered as a significant factor because it is the second contributor to k_{eff} uncertainty. This reaction cross-section has an 11.98% contribution to the total uncertainty of k_{eff} . This value is much higher in small-sized HTGRs than in other typical reactors [10, 20]. In addition, the elastic scattering of C-graphite is the third contributor, and the fission spectrum of ^{235}U is the fourth contributor.

It should be noted that the fuel pellet matrix materials are different between the pebble-bed and small-sized HTGRs: C-graphite is used for pebble-bed HTGRs and SiC for small-sized HTGRs. Furthermore, the volume ratio of Si in the small-sized HTGR fuel pellet was 55.87%, which was significantly higher than that in the pebble-bed reactor. For a more in-depth study on the effect of nuclear data in k_{eff} uncertainty under the CZP condition, some necessary nuclide reaction energy sensitivity coefficient curves are presented in Fig. 3.

Table 2 Top 10 nuclide reaction covariance contributors to k_{eff} uncertainty at CZP condition

Rank	Nuclide reaction		Nuclide reaction		Contributions to uncertainty in k_{eff} (% $\Delta k/k$)
1	^{235}U	ν	^{235}U	ν	$3.74 \times 10^{-1} \pm 2.90 \times 10^{-5}$
2	^{28}Si	n, γ	^{28}Si	n, γ	$2.58 \times 10^{-1} \pm 3.59 \times 10^{-6}$
3	C-graphite	elastic	C-graphite	elastic	$2.50 \times 10^{-1} \pm 4.64 \times 10^{-4}$
4	^{235}U	χ	^{235}U	χ	$1.80 \times 10^{-1} \pm 2.61 \times 10^{-4}$
5	^{235}U	n, γ	^{235}U	n, γ	$1.68 \times 10^{-1} \pm 2.22 \times 10^{-6}$
6	^{238}U	n, γ	^{238}U	n, γ	$1.47 \times 10^{-1} \pm 4.89 \times 10^{-6}$
7	^{235}U	n, f	^{235}U	n, γ	$1.32 \times 10^{-1} \pm 5.23 \times 10^{-6}$
8	^{235}U	n, f	^{235}U	n, f	$1.28 \times 10^{-1} \pm 9.49 \times 10^{-6}$
9	C-graphite	n, γ	C-graphite	n, γ	$9.14 \times 10^{-2} \pm 5.01 \times 10^{-7}$
10	^{157}Gd	n, γ	^{157}Gd	n, γ	$6.49 \times 10^{-2} \pm 5.23 \times 10^{-6}$

Fig. 3 (Color online) Important nuclide reaction energy sensitivity coefficients



As the first contributor to k_{eff} uncertainty under CZP conditions for small-sized HTGRs, the average number of neutrons emitted per fission event of ^{235}U has a large sensitivity coefficient in the thermal neutron energy range (energy less than 1 eV). Based on the “sandwich” rule, the large uncertainty contribution of the average number of neutrons emitted per fission event of ^{235}U can be attributed to its large sensitivity coefficient. The large k_{eff} uncertainty contribution of the radioactive capture reaction of ^{28}Si can be explained by the same reason. Additionally, C-graphite and ^{238}U as the resonance nuclides are mainly reflected in the resonance energy range (energy less than 0.1 MeV and more than 1 eV). Nevertheless, SU analysis in the CZP condition is just one stage of the depletion calculation. Next, the study focuses on the variation of the important nuclide reaction sensitivity coefficients and cross-section contributions on k_{eff} uncertainty during the full lifetime depletion calculation.

3.2 SU analysis of k_{eff} in the depletion calculation

3.2.1 k_{eff} sensitivity analysis

Generally, the k_{eff} sensitivity to important nuclide reactions can be used to measure the degree of influence of these reactions on k_{eff} . Here, we used RMC to evaluate the variations in the k_{eff} value and calculated the k_{eff} sensitivity to some important nuclide reactions during the full lifetime depletion process. The specific fuel burnup step times were

set as 0, 0.5, 1.5, 5, 20, 50, 100, 150, 200, 250, 300, 350, 400, 500, and 600 days. The k_{eff} results for these burnup steps are illustrated in Fig. 4. For the k_{eff} uncertainty quantification, in a condition of keep k_{eff} change trend during the full lifetime, select as few burnup step results as possible to reduce sensitivity coefficients calculation time. The 0, 5, 50, 150, 250, 400, and 600 days burnup step results were chosen for analysis.

During the depletion process in the RMC, the nuclide density required by the transport calculation was obtained from the solution of the depletion equation. In this way, the nuclide density is updated in each burnup step. Therefore, the nuclide density variation of certain important nuclides and their effect on k_{eff} uncertainty needs to be investigated. In general, some fission elements, fission products, and fission poison nuclides are considered, such as ^{235}U , ^{238}U , ^{239}Pu , ^{135}I , ^{135}Xe , ^{149}Sm , and ^{155}Gd . In the RMC Monte Carlo depletion calculation, nuclide density data are obtained from the results of the previous burnup step. Because the poison elements ^{135}Xe and ^{149}Sm are produced, as shown in Fig. 5, the large neutron absorption cross-section of these elements makes the k_{eff} decline steeply from the BOL to 5 days. Owing to the space self-shielding effect of the burnable poison Gd, k_{eff} exhibits an upward trend between 5 and 150 days. During the depletion, the burnable poison nuclide ^{155}Gd was consumed rapidly, and after nearly 250 days the amount in the reactor was very low, as illustrated in Fig. 5a. Therefore, without

Fig. 4 k_{eff} depletion results calculated by RMC

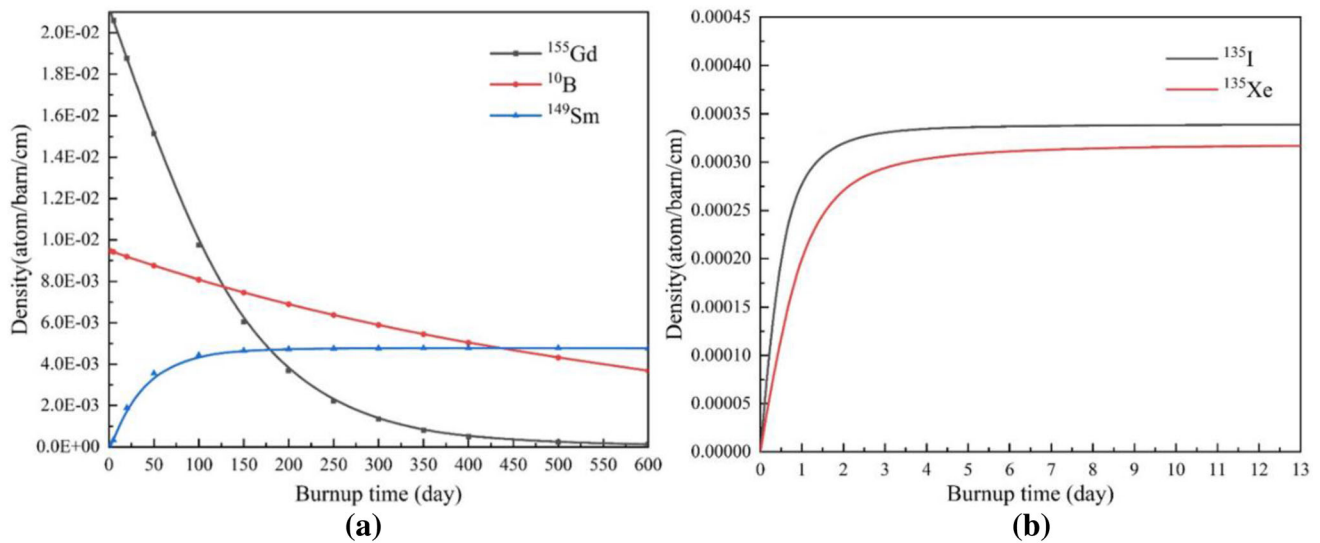
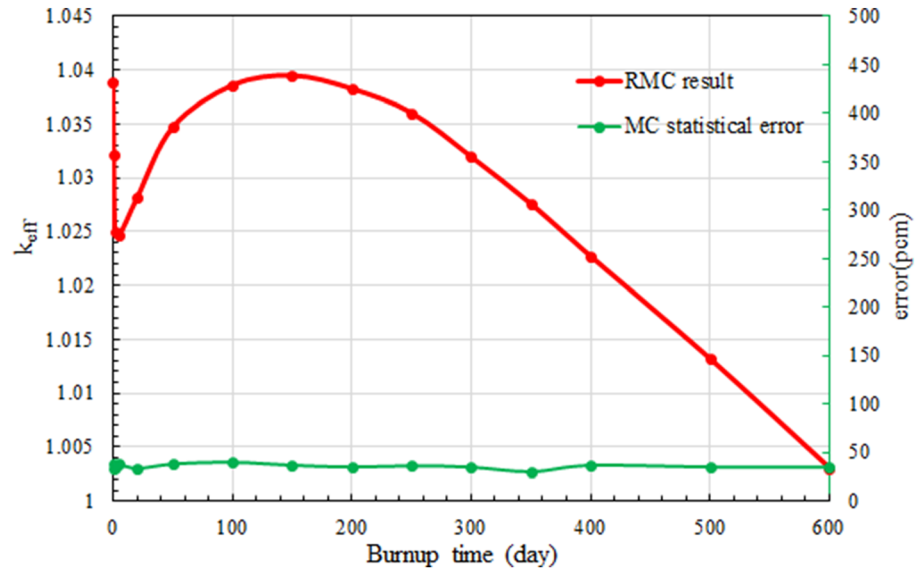


Fig. 5 Important nuclides density variation during the depletion calculation. **a** ^{155}Gd , ^{10}B and ^{149}Sm density variation; **b** ^{135}I and ^{135}Xe density variation

the effect of the burnable poison Gd, the k_{eff} value decreases with fuel depletion until the end of life.

According to the sensitivity analysis results, the k_{eff} sensitivity coefficients for some vital nuclide reactions were considerable during the depletion calculation. Table 3 lists the 14 main nuclide reactions with average integrated sensitivity coefficients during the small-sized HTGR depletion calculation. It should be noted that the average integrated sensitivity coefficients are calculated by integrating all energy groups for all regions and the sensitivity of the mixture materials through seven burnup steps. Two illustrative line charts of the integrated sensitivity coefficients of these important nuclides and their reaction cross sections are presented in Fig. 6. In addition, Fig. 7 shows

the difference in integrated sensitivity coefficients from the BOL to the end-of-life (EOL). According to Table 3 and Fig. 6, the integrated sensitivity coefficients of the average number of neutrons emitted per fission event of ^{235}U , elastic scattering of C-graphite, radioactive capture reaction of ^{239}Pu , and fission reaction of ^{239}Pu have more considerable variations than other nuclide reactions.

Moreover, the radioactive capture reaction of ^{28}Si has a relatively high sensitivity, and its sensitivity coefficient value essentially remains unchanged during the full life-time, as illustrated in Fig. 6. At the same time, the integrated sensitivity coefficients of some poison isotopes, such as ^{135}Xe , ^{149}Sm , and ^{155}Gd , have no obvious

Table 3 14 important nuclide reactions average integrate sensitivity coefficients

Nuclides	Nuclear reaction	Sensitivity coefficients	Spread (Max–Min)	STDEV (%)
^{235}U	ν	9.36×10^{-1}	1.37×10^{-1}	5.16
C-graphite	elastic	4.80×10^{-1}	1.32×10^{-1}	5.58
^{235}U	n,f	3.63×10^{-1}	3.04×10^{-2}	2.08
^{235}U	n, γ	-1.20×10^{-1}	6.87×10^{-3}	0.54
^{238}U	n, γ	-1.20×10^{-1}	3.36×10^{-3}	0.11
^{28}Si	n, γ	-5.54×10^{-2}	3.86×10^{-3}	0.15
^{239}Pu	n,f	3.33×10^{-2}	8.02×10^{-2}	3.05
^{239}Pu	n, γ	-2.23×10^{-2}	5.26×10^{-2}	2.02
^{135}Xe	n, γ	-1.24×10^{-2}	1.03×10^{-2}	0.55
^{10}B	n, γ	-7.72×10^{-3}	1.15×10^{-4}	0.02
^{157}Gd	n, γ	-6.49×10^{-3}	1.61×10^{-2}	0.69
^{149}Sm	n, γ	-4.68×10^{-3}	6.47×10^{-3}	0.29
^{155}Gd	n, γ	-2.66×10^{-3}	3.55×10^{-3}	0.19
^{235}U	χ	1.91×10^{-10}	1.57×10^{-10}	0.00

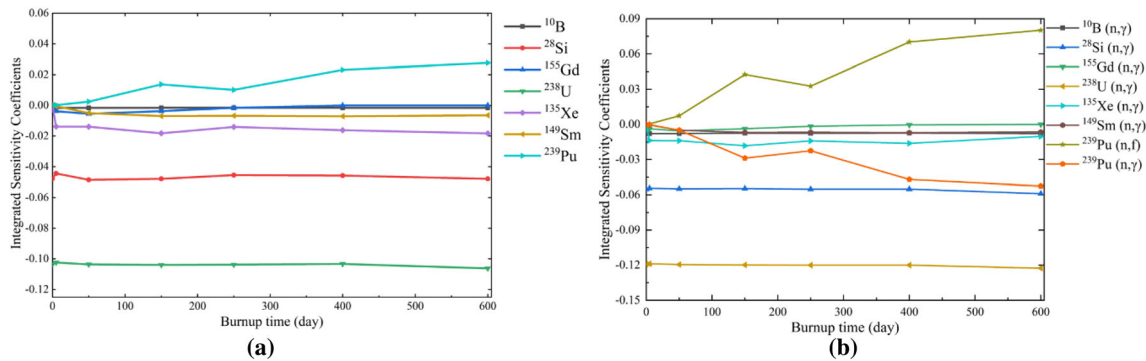


Fig. 6 (Color online) Integrated sensitivity coefficients of important nuclides and their cross sections. (a) Important nuclides integrated sensitivity coefficients; (b) Important nuclide cross sections integrated sensitivity coefficients

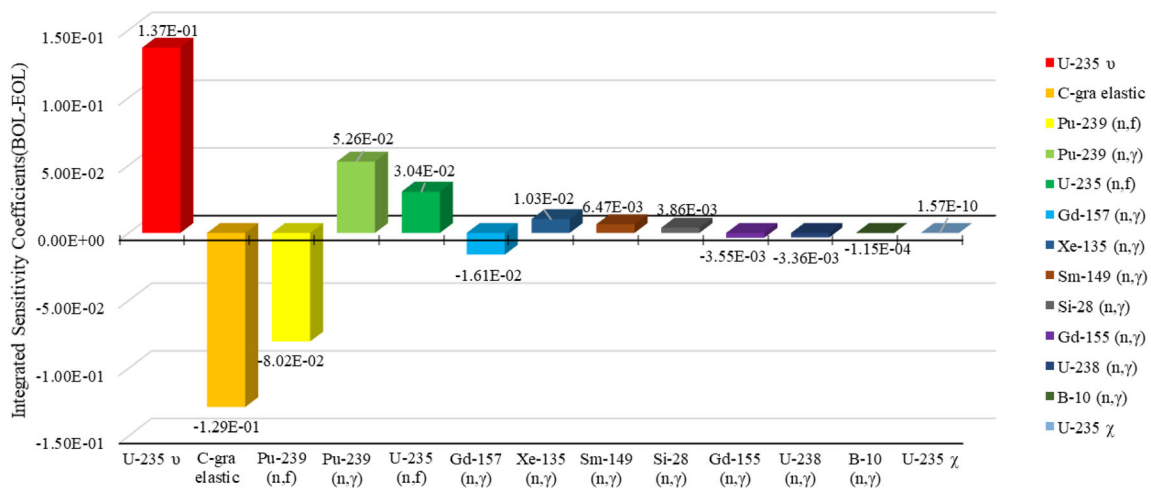


Fig. 7 (Color online) Integrated sensitivity coefficients variation (BOL-EOL) of important nuclide reactions

variation, and these values are quite small during the full lifetime depletion.

3.2.2 k_{eff} uncertainty analysis

According to the previous analysis of the important nuclide reaction sensitivity coefficients, the uncertainty contributions of the reaction cross sections to k_{eff} may have significantly different throughout the depletion calculation, which requires further study. The SU results calculated by RMC show that the rank of the top eight contributors during the full lifetime depletion calculation did not differ substantially, however the contribution values varied. There are 12 important nuclide reaction cross-section average contributions to the k_{eff} uncertainty for the small-sized HTGR depletion calculation, which are illustrated in Table 4. These contributions to the k_{eff} uncertainty are the average values of the results of the seven burnup steps. It is obvious that the elastic scattering of C-graphite, radioactive capture of ^{135}Xe , radioactive capture of ^{157}Gd , radioactive capture and fission reaction of ^{239}Pu , and the average number of neutrons emitted per fission event of ^{235}U change substantially throughout the depletion calculation through the standard deviation presented in Table 4. In addition, combined with the results summarized in Tables 3 and 4, the radioactive capture reactions of poison isotopes ^{157}Gd and ^{135}Xe have relatively large variations in contribution values. However, their sensitivity coefficients were mostly stable during the lifetime depletion calculation.

The 12 important nuclide reaction cross-sectional contributions to k_{eff} uncertainty in small-sized HTGR depletion calculations are shown in Fig. 8. The solid lines

represent the uncertainty contribution variations of the nuclear reaction for each nuclide that exists at the BOL. The figure shows that the average number of neutrons emitted per fission event of ^{235}U contributions decreased with the depletion calculation, but it was still the most significant contributor to the uncertainty of k_{eff} across the full lifetime. Furthermore, all cross sections other than the elastic scattering cross section of C-graphite and the radioactive capture cross section of ^{28}Si exhibited a downward trend. In particular, the radioactive capture reaction of ^{157}Gd showed a noticeable decline from BOL to nearly 150 days. This was mainly caused by the depletion of ^{157}Gd . Simultaneously, this also led to a reduction in the average number of neutrons emitted per fission event of ^{235}U , contributing to k_{eff} uncertainty.

The dotted lines in Fig. 8 express the fission product reaction contribution to k_{eff} uncertainty; all reaction contributions have an increasing trend with the nuclides produced during the burnup calculation. As an important fission product, ^{135}Xe is produced rapidly at the BOL and reaches equilibrium at 4 to 5 days. Simultaneously, the radioactive capture reaction of ^{135}Xe was the main contributor to fission products until nearly 450 days. After 450 days, the fission reaction and radioactive capture cross-section of ^{239}Pu became the main contributors. However, the contributions of the radioactive capture reaction of ^{149}Sm were low and barely changed.

Figure 9 shows the total variation of the important nuclide reaction contributions to the k_{eff} uncertainty. The phenomenon concluded with Tables 3 and 4 can be more intuitively seen in Fig. 7 and Fig. 9 that the radioactive capture of ^{135}Xe and ^{157}Gd has only tiny variations in

Table 4 12 important nuclide reactions average contributions to the k_{eff} uncertainty

Nuclides	Covariance matrix		Average contributions to uncertainty in k_{eff} (% $\Delta k/k$)	Spread (Max–Min)	STDEV (%)
	Nuclide reaction	Nuclide reaction			
^{235}U	ν	ν	3.50×10^{-1}	6.98×10^{-2}	2.58
^{28}Si	n, γ	n, γ	2.59×10^{-1}	1.33×10^{-2}	0.52
C-graphite	elastic	elastic	2.57×10^{-1}	6.59×10^{-2}	2.90
^{235}U	χ	χ	1.67×10^{-1}	2.49×10^{-2}	0.99
^{235}U	n, γ	n, γ	1.56×10^{-1}	2.10×10^{-2}	1.00
^{238}U	n, γ	n, γ	1.48×10^{-1}	4.43×10^{-3}	0.17
^{235}U	n,f	n, γ	1.21×10^{-1}	1.02×10^{-2}	0.78
^{135}Xe	n, γ	n, γ	5.13×10^{-2}	4.26×10^{-2}	2.48
^{157}Gd	n, γ	n, γ	2.50×10^{-2}	6.45×10^{-2}	2.95
^{239}Pu	n,f	n,f	2.41×10^{-2}	4.42×10^{-2}	2.26
^{239}Pu	n, γ	n, γ	2.28×10^{-2}	4.97×10^{-2}	2.12
^{149}Sm	n, γ	n, γ	7.23×10^{-3}	3.24×10^{-3}	0.40

Fig. 8 Important nuclide reaction contribution variations to uncertainty in k_{eff}

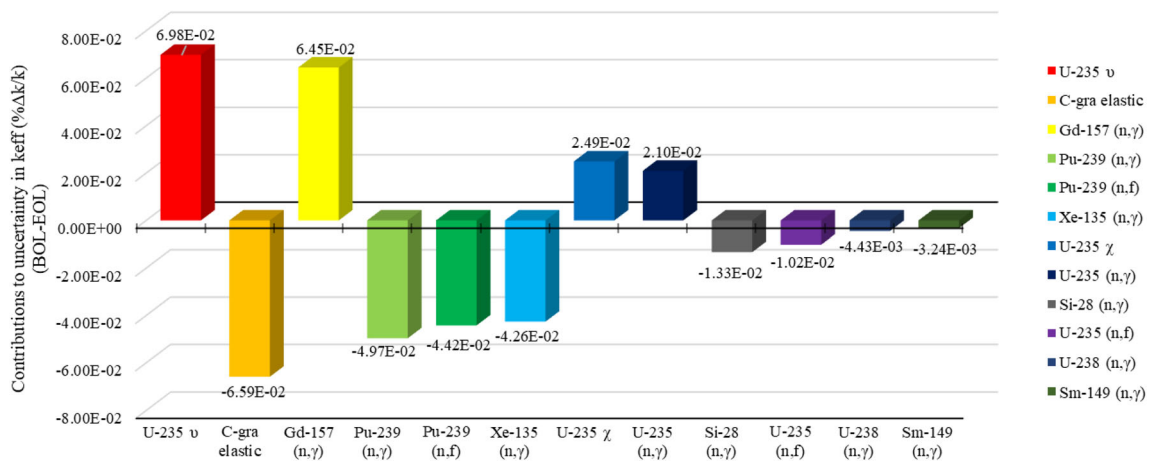
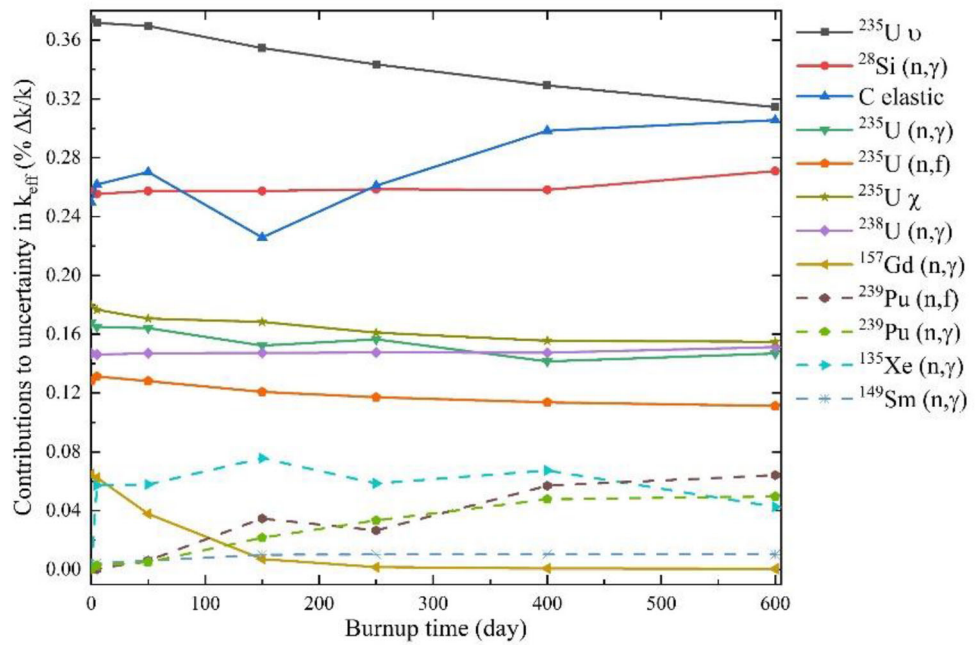


Fig. 9 (Color online) Important nuclide reaction contribution variations (BOL-EOL) to uncertainty in k_{eff}

sensitivity coefficients, but the contributions to k_{eff} uncertainty differ significantly during the full lifetime.

Considering the numerical results in Sect. 3.2.1, the fission spectrum of ^{235}U makes a large contribution to k_{eff} uncertainty after the radioactive capture of ^{135}Xe and ^{157}Gd . However, the sensitivity coefficients do not noticeably increase during the depletion calculation. However, the nuclide reaction cross-section has uncertainty, which is presented by the covariance matrix based on the nuclear data library [23]. Because the “sandwich” rule is used to quantify uncertainty, although the integrated sensitivity of k_{eff} to the ^{235}U fission spectrum is only -1.91×10^{-10} , the large relative covariance explains why the ^{235}U fission spectrum is the fourth most significant contributor. In addition, the relative covariance of the

radioactive capture reaction of ^{28}Si is not large in the ENDF/B-VII.1 covariance library [23], but its contribution to the uncertainty of k_{eff} is still significant in small-sized HTGR depletion calculations. The density of ^{28}Si remained almost unchanged throughout the lifetime. Thus, it can be concluded that the large volume ratio in the core and large average sensitivity coefficient are the main reasons that the radioactive capture of ^{28}Si is the second largest contributor to k_{eff} uncertainty.

After analyzing the contribution of some important nuclide reactions, the total uncertainty of k_{eff} during the full lifetime depletion calculation was quantified, as shown in Fig. 10. According to the numerical results of the seven burnup steps, the uncertainty of k_{eff} remained largely constant. Moreover, owing to the fission products

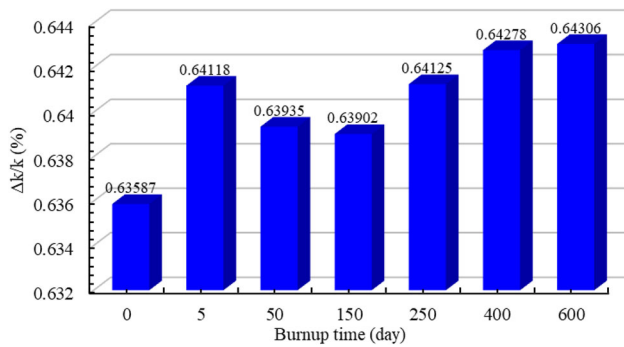


Fig. 10 Total uncertainty of k_{eff} during the full lifetime depletion calculation

constantly generated during the depletion process, the uncertainty has a slightly increasing trend.

Since 2007, there have been many developments in reactor uncertainty analysis modeling, such as the OECD/NEA of Light Water Reactor (LWR) UAM, OECD/NEA of Boiling Water Reactor (BWR) UAM, and IAEA CRP UAM on HTGR [7, 9, 20, 21]. The k_{eff} uncertainty results of these reactor uncertainty analysis projects are presented in Table 5. The burnup value of the small-sized HTGR was only 10.789 GWd/tU at EOL. Nevertheless, the burnup of PWR and HTR-10 was much deeper. At the same time, the PWR and BWR all have an extensive increase in k_{eff} uncertainty during the full lifetime depletion, and the uncertainty value increased by 28.98% and 40.22%, respectively. However, the uncertainty of k_{eff} in small-sized HTGRs only increased by 1.12% in the full lifetime depletion calculation owing to the low discharge burnup design.

After analyzing the k_{eff} uncertainty due to the nuclear data during the burnup calculations for different types of reactors, the contributions of the top five most important nuclide reactions to k_{eff} uncertainty in different typical reactors under CZP conditions were determined, as illustrated in Table 6. BWR, pebble-bed HTR-10, and small-sized HTGRs were included. It is clear that in BWR, the top contributor to k_{eff} uncertainty is the radioactive capture reaction of ^{238}U . However, in the two HTGRs, the first contributor to k_{eff} uncertainty was the average number of neutrons emitted per fission event of ^{235}U . Moreover, the radioactive capture reaction of ^{28}Si being the second

contributor to k_{eff} uncertainty is a novel finding in small-sized HTGRs.

4 Mechanism analysis of k_{eff} uncertainty

From the above SU analysis during the small HTGR depletion calculation, it was revealed that some cross sections of ^{235}U , ^{28}Si , ^{157}Gd , C-graphite, ^{239}Pu , ^{135}Xe , and ^{149}Sm had high sensitivity coefficients or significant contributions to the uncertainty of k_{eff} . The reason that the radioactive capture reaction cross section of ^{28}Si has such a large contribution to the uncertainty of k_{eff} was investigated in Sect. 3.2.2. Additionally, other changes in significant nuclide reaction sensitivity coefficients may directly affect the uncertainty of k_{eff} during the full lifetime depletion process. Therefore, it is necessary to carry out further mechanistic analyses.

Based on the results in Sect. 3, the average number of neutrons emitted per fission event, fission spectrum, radioactive capture reaction, and fission reaction of ^{235}U all have a significant contribution to k_{eff} uncertainty during the depletion calculation. As one of the most important elements in fission reactors, the nuclear data of ^{235}U have a significant effect on k_{eff} uncertainty and are valuable for further studies.

According to the uncertainty quantification method introduced in Sect. 2, the uncertainty of k_{eff} due to nuclear data depends on its covariance data and sensitivity coefficients. The four crucial reactions of the ^{235}U integrated sensitivity coefficients and their contribution to k_{eff} uncertainty are presented in Fig. 11. From these two histograms, it is noteworthy that the high sensitivity of the average number of neutrons emitted per fission event of ^{235}U directly leads to a large ^{235}U contribution to k_{eff} uncertainty. Although other crucial reactions of ^{235}U also significantly contribute to the total uncertainty of k_{eff} , the k_{eff} sensitivities to these reactions are not very significant and only slightly decrease during the full lifetime. In addition, the sensitivity coefficients of the ^{235}U fission spectrum are too small to be observed in this histogram, however the contribution to k_{eff} uncertainty is still large due to the high relative covariance data [23]. However, the uncertainties of the average number of neutrons emitted per fission event and fission reaction, which are based on the

Table 5 Different reactor k_{eff} uncertainty due to the nuclear data

Reactor	EOL burnup (GWd/tU)	k_{eff} uncertainty (% $\Delta k/k$)	
		BOL	EOL
PWR TMI-1	60	0.49	0.69
BWR PB-2	45	0.55	0.92
HTR-10	52.72	0.6609	–
Small-sized HTGR	10.789	0.6359	0.6431

Table 6 Different reactor top 5 important reaction contributions to k_{eff} uncertainty at CZP condition

Rank	BWR		%Δk/k	HTR-10		%Δk/k	Small-sized HTGR		%Δk/k
	Nuclide reaction			Nuclide reaction			Nuclide reaction		
1	^{238}U (n, γ)	^{238}U (n, γ)	0.30	^{235}U υ	^{235}U υ	0.38	^{235}U υ	^{235}U υ	0.37
2	^{235}U υ	^{235}U υ	0.28	C-gra elastic	C-gra elastic	0.31	^{28}Si (n, γ)	^{28}Si (n, γ)	0.26
3	^{235}U (n, γ)	^{235}U (n, γ)	0.14	^{235}U χ	^{235}U χ	0.25	C-gra elastic	C-gra elastic	0.25
4	^{235}U (n, f)	^{235}U (n, f)	0.14	C-gra (n, γ)	C-gra (n, γ)	0.19	^{235}U χ	^{235}U χ	0.18
5	^{235}U (n, f)	^{235}U (n, γ)	0.12	^{235}U (n, γ)	^{235}U (n, γ)	0.18	^{235}U (n, γ)	^{235}U (n, γ)	0.17

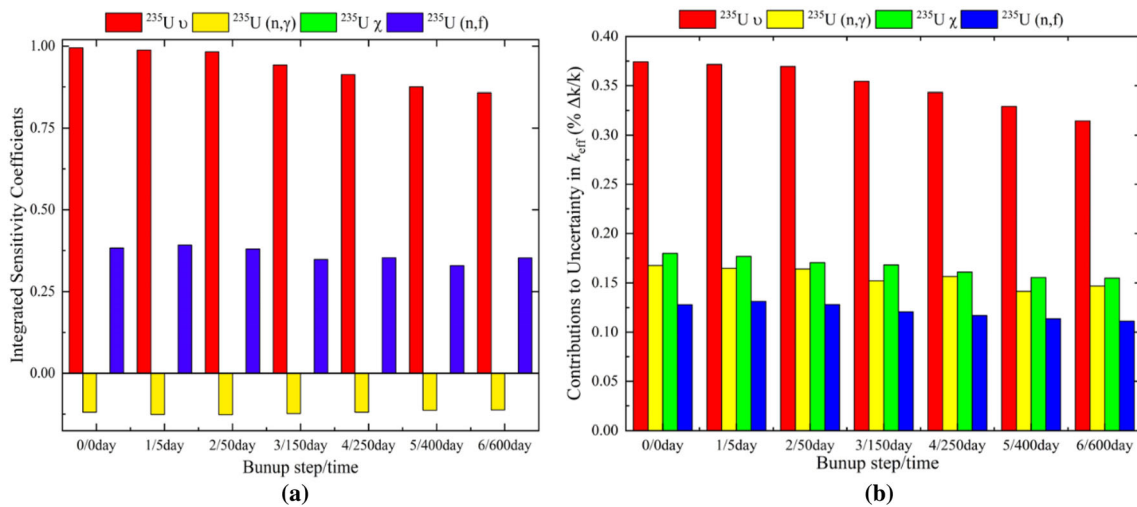


Fig. 11 (Color online) ^{235}U important reactions integrated sensitivity coefficients and contribution to k_{eff} uncertainty. (a) ^{235}U important reactions integrated sensitivity coefficients; (b) ^{235}U important reaction’s contribution to k_{eff} uncertainty

covariance matrices, are much smaller [23]. Therefore, the average number of neutrons emitted per fission event and fission reaction of ^{235}U has a large amount of uncertainty, which can be attributed to their large sensitivity coefficients.

Furthermore, the elastic scattering of C-graphite, the radioactive capture reaction, and the fission reaction of ^{239}Pu also have considerable impact and variation during the depletion process. The integrated sensitivity coefficients of these two important nuclides are shown in Fig. 12. In these two histograms, the elastic scattering of C-graphite has a large basal sensitivity during the full lifetime and even exhibits a slight growth at EOL. This trend also reflects the total uncertainty change in k_{eff} to some extent. At the same time, the two important reactions of ^{239}Pu sensitivity coefficients have a significant growth at EOL, but their sensitivity coefficient values are still slight compared with those of C-graphite and ^{235}U . Based on this finding, the reason that the radioactive capture and fission reactions do not contribute significantly to k_{eff} uncertainty at EOL can be explained clearly. Moreover, this

phenomenon explains why the total k_{eff} uncertainty does not increase significantly at EOL.

Fission poison products, such as ^{135}Xe and ^{149}Sm , are generated during the full lifetime depletion process. These nuclides dramatically affect k_{eff} due to their substantial absorption cross sections and therefore, the impact of these poison nuclide reaction cross-sections on k_{eff} uncertainty should be studied. The integrated sensitivity coefficients of the radioactive capture reaction of ^{135}Xe , ^{149}Sm , and ^{157}Gd during the depletion calculation are shown in Fig. 13. Interestingly, based on the rapid production of ^{135}Xe at the BOL, the integrated sensitivity coefficients of ^{135}Xe increased significantly at 5 days and reached the highest value at 150 days. The integrated sensitivity coefficients of ^{149}Sm have slightly increased at 5 days and also get peak at 150 days, but its integrated sensitivity values are much lower than that of ^{135}Xe . The burnable poison material ^{157}Gd is input at the BOL. Its sensitivity coefficients show an obvious decrease after 150 days and nearly decrease to zero at EOL. After 150 days, the main contributor of poison elements was ^{135}Xe in the small-sized HTGR.

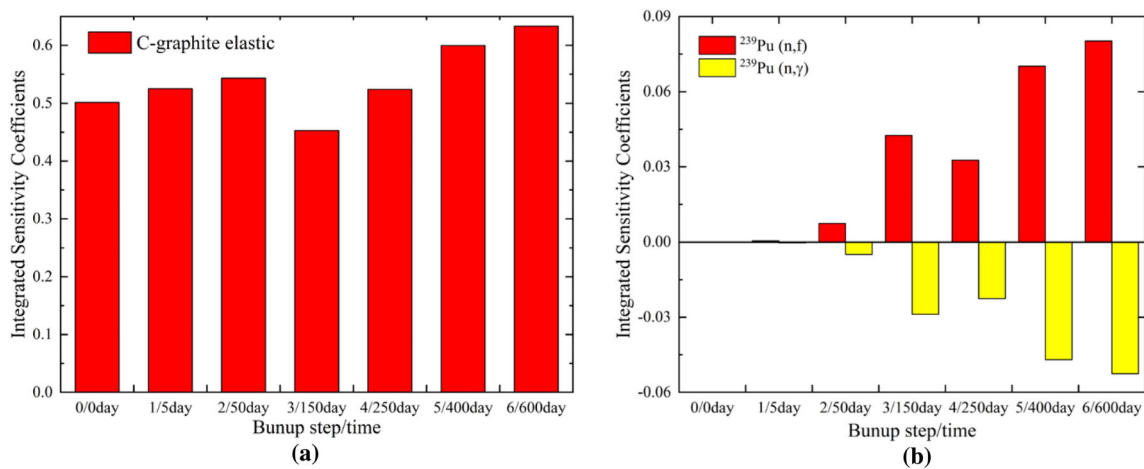
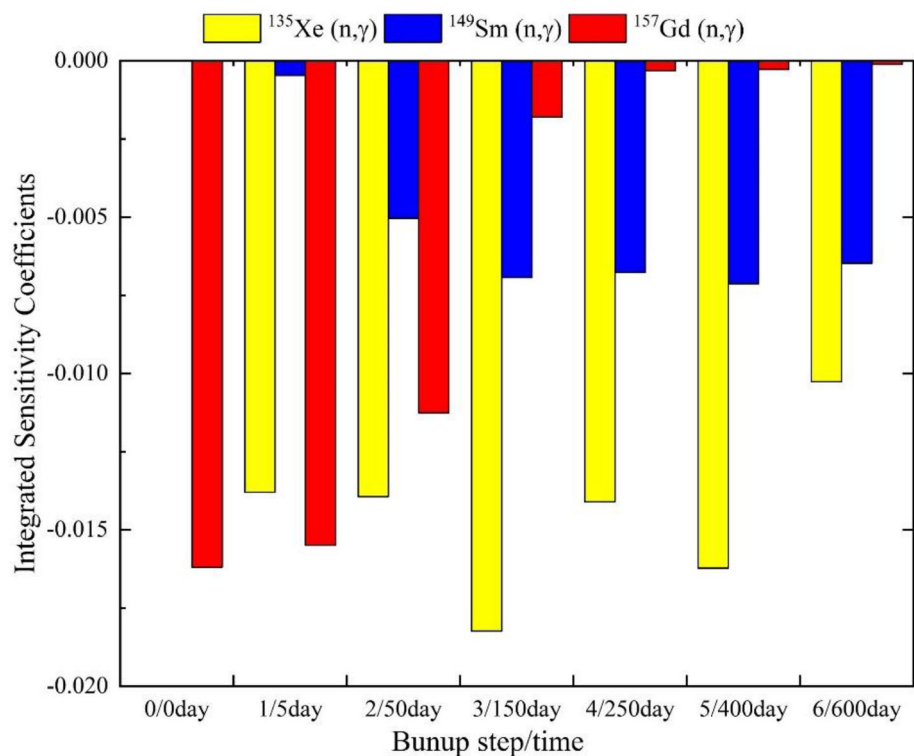


Fig. 12 (Color online) Integrated sensitivity coefficients of C-graphite and ^{239}Pu . (a) C-graphite elastic scattering integrated sensitivity coefficients; (b) ^{239}Pu radioactive capture reaction and fission reaction integrated sensitivity coefficients

Fig. 13 (Color online) Sensitivity coefficients of the poison elements



However, the integrated sensitivity coefficients of these poison elements are still much smaller than those of C-graphite or ^{235}U . Therefore, based on the analysis results and the “sandwich” rule, the contributions to k_{eff} uncertainty of these main poison nuclide reactions in small-sized HTGRs arise from their relative covariances.

5 Conclusion

In this study, the k_{eff} uncertainties due to the nuclear data in the CZP condition and full lifetime depletion calculation were quantified for a small-sized HTGR. RMC was used to generate the small-sized HTGR high-fidelity model and carry out critical calculations and for depletion and uncertainty calculations. In the depletion calculation, the predictor correction method was applied. In addition, the CLUTCH method was used for sensitivity analysis, and the “sandwich” method was utilized to quantify the k_{eff}

uncertainty through the ENDF/B-VII.1 covariance data. Our main findings are as follows:

First, the uncertainty of k_{eff} due to nuclear data at the CZP condition was considered. According to SU results in the CZP condition, the average number of neutrons emitted per fission event of ^{235}U is the most important contributor to the uncertainty of k_{eff} . The radioactive capture reaction of ^{28}Si is the second largest contributor to the uncertainty in k_{eff} because of its heavy volume ratio in the fuel pellet. This finding differs from the results of our study of the pebble-bed HTGR [10]. The total uncertainty of k_{eff} due to the nuclear data at the CZP condition was approximately 636 pcm.

Second, the 24 fuel zone model was used for the full lifetime depletion calculation. According to the results illustrated in Tables 2 and 4, the top eight most important nuclide reaction contributors themselves to k_{eff} uncertainty did not change across the full lifetime. However, the k_{eff} uncertainty from the radioactive capture and fission reactions of ^{239}Pu increased significantly at EOL. Simultaneously, other types of reactors, such as PWR, BWR, and pebble bed HTGR, were compared with the small-sized HTGR in the full lifetime depletion k_{eff} uncertainty quantification. The results showed that the small-sized HTGR had a lower burnup value at EOL, and its k_{eff} uncertainty only changed slightly during the full lifetime depletion calculation. In the small-sized HTGR, the uncertainty of k_{eff} during the full lifetime increased by 1.1196%, compared to 28.9855% for PWR and 40.2174% for BWR.

Finally, the variation in k_{eff} uncertainty due to nuclear data during the full lifetime depletion was analyzed. The average number of neutrons emitted per fission event of ^{235}U and elastic scattering of C-graphite significantly contribute to the uncertainty of k_{eff} owing to their large sensitivity coefficients. However, this conclusion is contrary to the fission spectrum of ^{235}U , in which the significant contribution to the k_{eff} uncertainty is due to the large covariance data of itself. Moreover, ^{239}Pu is one of the main fission products, and its important reaction cross-sectional contributions to k_{eff} uncertainty increased at EOL, but did not surpass the contributions of ^{235}U or C-graphite owing to its small sensitivity coefficient. This is the key reason that the total uncertainty of k_{eff} grew little at the EOL. In addition, the poison elements, ^{135}Xe , ^{149}Sm , and ^{157}Gd , were investigated in the depletion calculation. The k_{eff} sensitivity coefficients for the poison element cross sections varied significantly during the full lifetime, as illustrated in Fig. 13. These changes have an obvious influence on the k_{eff} value but did not significantly affect the k_{eff} uncertainty.

In general, the k_{eff} uncertainty due to nuclear data was quantified, and some important nuclides and reactions were determined to contribute significantly to the k_{eff}

uncertainty. These findings are valuable for the design and optimization of new small-sized prismatic HTGRs. However, the nuclear data introduces non-negligible uncertainties to the nuclide density, which further contributes to the uncertainty of k_{eff} during the depletion process. This work is now in progress, and the uncertainty results will be reported in the following papers.

Author contributions All authors contributed to the study conception and design. Material preparation, data collection and analysis were performed by Rong-Rui Yang, Yuan Yuan, Chen Hao, Ji Ma and Guang-Hao Liu. The first draft of the manuscript was written by Rong-Rui Yang and Chen Hao, and all authors commented on previous versions of the manuscript. All authors read and approved the final manuscript.

References

- Z.X. Wu, Safety features of modular high temperature gas-cooled reactors (MHTGR). *Tsinghua Sci. Technol.* **1**, 8–11 (1996)
- X.C. Zhang, D. She, F.B. Chen et al., Temperature analysis of the HTR-10 after full load rejection. *Nucl. Sci. Tech.* **30**, 163 (2019). <https://doi.org/10.1007/s41365-019-0692-1>
- F. Gou, Y. Liu, F.B. Chen et al., Thermal behavior of the HTR-10 under combined PLOFC and ATWS condition initiated by unscrambled control rod withdrawal. *Nucl. Sci. Tech.* **29**, 123 (2018). <https://doi.org/10.1007/s41365-018-0472-3>
- D. She, B. Xia, J. Guo et al., Prediction calculations for the first criticality of the HTR-PM using the PANGU code. *Nucl. Sci. Tech.* **32**, 90 (2021). <https://doi.org/10.1007/s41365-021-00936-5>
- P.M. Williamms, F.A. Silady, T.D. Dunn et al., MHTGR development in the United States. *Prog. Nucl. Energ.* **28**, 265–346 (1994). [https://doi.org/10.1016/0149-1970\(94\)90002-7](https://doi.org/10.1016/0149-1970(94)90002-7)
- F. Reitsma, W. Kim, The contribution of cross section uncertainties to pebble bed reactor eigenvalues results: IAEA cooperative research project phase I stand alone neutronics. Paper presented at the PHYSOR2016 Conference (Sun Valley, Idaho, USA 1 May. 2016).
- F. Reitsma, G. Strydom, B. Tyobeka et al., The IAEA coordinated research program on HTGR reactor physics, thermal-hydraulics and depletion uncertainty analysis: description of the benchmark test cases and phases. Paper presented at the HTR2012 Conference (Tokyo, Japan 2012).
- F. Bostelmann, G. Strydom, F. Reitsma et al., The IAEA coordinated research program on HTGR uncertainty analysis: phase I status and Ex. I-1 prismatic reference results. *Nucl. Eng. Des.* **306**, 77–88 (2016). <https://doi.org/10.1016/j.nucengdes.2015.12.009>
- G. Strydom, IAEA Coordinated Research Project on HTGR Physics, Thermal-Hydraulics, and Depletion Uncertainty Analysis Prismatic HTGR Benchmark Specification: Phase II. Idaho National Laboratory, Technical Report INL/EXT-18-44815 (2018). <https://doi.org/10.2172/1467563>
- C. Hao, Y.Y. Cheng, J. Guo et al., Mechanism analysis of the contribution of nuclear data to the k_{eff} uncertainty in the pebble bed HTR. *Ann. Nucl. Energy* **120**, 857–868 (2018). <https://doi.org/10.1016/j.anucene.2018.07.015>
- Y.H. Tae, H.C. Lee, Y.C. Jin et al., Improvement and application of DeCART/MUSAD for uncertainty analysis of HTGR neutronic parameters. *Nucl. Eng. Technol.* **52**, 461–468 (2020). <https://doi.org/10.1016/j.net.2019.08.006>

12. M. L. Williams, *Perturbation Theory for Nuclear Reactor Analysis*, ed. by Y. Ronen (Boca Raton, Florida, 1986).
13. C.M. Perfetti, *Doctoral Dissertation (Advanced Monte Carlo Methods for Eigenvalue Sensitivity Coefficient Calculation*. University of Michigan 2012). <http://hdl.handle.net/2027.42/93973>
14. M. Pusa, Incorporating sensitivity and uncertainty analysis to a lattice physics code with application to CASMO-4. *Ann. Nucl. Energ.* **40**, 153–162 (2012). <https://doi.org/10.1016/j.anucene.2011.10.013>
15. A. Arzhannikov, S. Bedenko, V. Shmakov et al., Gas-cooled thorium reactor at various fuel loadings and its modification by a plasma source of extra neutrons. *Nucl. Sci. Tech.* **30**, 181 (2019). <https://doi.org/10.1007/s41365-019-0707-y>
16. K.V.V. Devi, J.N. Dubey, J. Gupta et al., TRISO fuel volume fraction and homogeneity: a nondestructive characterization. *Nucl. Sci. Technol.* **30**, 41 (2019). <https://doi.org/10.1007/s41365-019-0573-7>
17. K. Wang, Z.G. Li, D. She et al., RMC—a Monte Carlo code for reactor core analysis. *Ann. Nucl. Energy* **82**, 121–129 (2015). <https://doi.org/10.1016/j.anucene.2014.08.048>
18. W.L. Li, G.L. Yu, K. Wang et al., Comparative analysis of coupling schemes of Monte Carlo burnup calculation in RMC. *Ann. Nucl. Energy* **137**, 107024 (2020). <https://doi.org/10.1016/j.anucene.2019.107024>
19. G.L. Shi, Y.C. Guo, C.L. Jia et al., Improvement of sensitivity and uncertainty analysis capabilities of generalized response in Monte Carlo code RMC. *Ann. Nucl. Energy* **154**, 108099 (2021). <https://doi.org/10.1016/j.anucene.2020.108099>
20. W. Zwermann, A. Aures, L. Gallner et al., Nuclear data uncertainty and sensitivity analysis with XSUSA for fuel assembly depletion calculations. *Nucl. Eng. Technol.* **46**, 343–352 (2014). <https://doi.org/10.5516/NET.01.2014.711>
21. K. Ivanov, M. Avramova, I. Kodeli, Benchmark for Uncertainty Analysis in Modeling (UAM) for Design, Operation and Safety Analysis of LWRs. Volume 1- Specification and Supporting Data for the Neutronics Cases (Phase I) Version 1.0, Technical report, NEA/NSC/DOC23 (2007). <https://www.oecdnea.org/science/docs/2007/nsc-doc2007-23>
22. C. Hao, Y.Y. Cheng, Q.C. Teng, Quantification and mechanism analysis of the k_{inf} uncertainty propagated from nuclear data for the TRISO particle fuel pebble. *Ann. Nucl. Energ.* **127**, 248–256 (2019). <https://doi.org/10.1016/j.anucene.2018.12.011>
23. M.B. Chadwick, M. Herman, P. Oblozinsky et al., ENDF/B-VII.1 nuclear data for science and technology: cross sections, covariance, fission product yields and decay data. *Nucl. Data Sheets* **112**, 2887–2996 (2011). <https://doi.org/10.1016/j.nds.2011.11.002>